Efficient iridium catalysts for base-free hydrogenation of levulinic acid

S. Wang,[a] H. Huang,[a] V. Dorcet,[b] T. Roisnel,[b] C. Bruneau,[a] C. Fischmeister[a]*

[a] Institut des Sciences Chimiques de Rennes, UMR 6226 CNRS, Université de Rennes 1, Organometallics: Materials and Catalysis, Centre for Catalysis and Green Chemistry. Campus de Beaulieu, F-35042 Rennes Cedex, France

cedric.fischmeister@univ-rennes1.fr

[b] Centre de Diffractométrie X

Institut des Sciences Chimiques de Rennes UMR 6226 CNRS, Université de Rennes 1, F-35042 Rennes Cedex, France

KEYWORDS: Homogeneous catalysis, ruthenium, iridium, transfer hydrogenation, hydrogenation, levulinic acid, γ-valerolactone

ABSTRACT

The synthesis and characterization of new dicationic ruthenium and iridium complexes bearing a dipyridylamine ligand (dpa) is reported. These complexes display an unusual zwitterionic molecular structure in the solid state. The iridium complex [Cp*Ir(dpa)(OSO_3)] **Ir1** was found to be very efficient in base free hydrogenation of levulinic acid into γ–valerolactone (GVL). TON

as high as 174000 in hydrogenation have been obtained. We have demonstrated that reduction of LA into GVL by "transfer hydrogenation" with formic acid is in fact operating by hydrogenation fed by preliminary formic acid dehydrogenation. A mechanism based on the characterization and isolation of Ir-H complexes is proposed.

INTRODUCTION

Reduction processes play a crucial role in organic syntheses both in academia and industry. Many efficient and selective transformations have been discovered leading to tremendous developments and implementation of reduction transformations. The growing demand for biosourced compounds is currently fostering the demand for efficient and robust catalysts able to address the transformation of polyfunctional biosourced chemicals into useful chemicals.[1] Levulinic acid (LA), one of the biosourced platform chemical has received a strong interest as precursor of a variety of biosourced compounds with a broad range of applications.[2] One specific application concerns the reduction of levulinic acid into γ-valerolactone (GVL), a chemical with multiple utilities.[3] The synthesis of GVL hence represents an intrinsic interest as useful biosourced compounds but it is also a challenging transformation for the design and development of reduction catalysts with enhanced performances that could be implemented in other reduction reactions not necessarily involving renewables. Homogeneous and heterogeneous catalysts have been reported for the efficient reduction of LA into GVL. Heterogeneous catalysts are undoubtedly interesting for their easy separation procedures and for the possibility to operate under continuous flow but their activity is usually low and they require high reaction temperatures, typically higher than 150 °C.[4] In 1977, Joó reported the homogeneous hydrogenation of levulinic acid with ruthenium complexes.[5] Since then, a number of homogeneous catalysts with improved performances have been reported of which ruthenium and

iridium complexes led to the best results.[6] In hydrogenation, Mika reported a TON of 12740 with a [Ru(acac)$_3$]/DPPB catalyst operating under solvent and additive free conditions but at a rather high temperature and pressure of 140 °C and 100 bar, respectively.[7] Zhou reported an impressive TON of 71000 obtained with an iridium trihydride pincer catalyst. The reaction could be run at 100 °C, but a high pressure of hydrogen was required (100 bar) and the addition of 1.2 equivalent of base was necessary.[8] Another iridium catalyst reported by Fu reached a higher TON of 78000 under different reaction conditions (120 °C, 10 bar H_2) without additive.[9] Transfer hydrogenation processes have received less attention despite the perspective of running the reaction with formic acid (FA) as reducing agent which is a co-product of LA synthesis from carbohydrate acidic depolymerization.[10] The transfer hydrogenation of LA was reported with a TON as high as 2400 by Horvàth using the bifunctional Shvo catalyst[11] and a TON of 9800 by Fu with an iridium catalyst.[9] Both systems operate under additive free conditions. Recently, following previous results on the synthesis of dipyridylamine-containing ruthenium catalysts,[12a] we have reported new ruthenium and iridium complexes for the transfer hydrogenation of LA into GVL.[12b] TONs up to 2760 were obtained, but unlike transformations using Shvo's catalyst, these catalysts required a base which limits their potential developments. In this manuscript we present our latest developments on the synthesis, characterization and catalytic performances of new ruthenium and iridium complexes operating under base free conditions.

RESULTS AND DISCUSSION

Synthesis and characterization of new complexes

We previously reported the cationic ruthenium chloride and iridium chloride complexes **A** and **B** bearing dipyridylamine ligands (dpa) (Scheme 1). These complexes were efficient in the

transfer hydrogenation of LA with FA provided two equivalents of triethylamine were added to the reaction mixture. These complexes were also found to be poor hydrogenation catalysts.[12b] This latter result could find its origin in the absence of free coordination site thus preventing the formation of a dihydrogen complex intermediate precursor of metal hydride or dihydride species.[13] Recently, numerous dicationic metal-bipyridine complexes in particular proton-responsive complexes of the general formula $[Cp^*Ir(bpy)H_2O)]SO_4$ have been used in various reduction reactions.[14, 15] Inspired by these chloride free catalysts bearing a labile aquo-ligand we attempted the synthesis of the dicationic version of complexes **A** and **B** (Scheme 1). Having already prepared **A** and **B**, the new complexes **Ru1**, **Ir1** and **Ir2** were synthesized by abstraction of the chloride ligand with silver sulfate. To our surprise, the complexes were not isolated as dicationic aquo-complexes as reported in the literature for Cp*Ir(bipyridine) complexes but as a zwitterionic complexes bearing a coordinated sulfato-ligand as evidenced by X-ray analysis of crystals grown in a mixture of $MeOH/Et_2O$ (Figure 1). In fact, previously reported bipyridine containing complexes $[Cp^*Ir(bpy)(OH_2][SO_4]$ were prepared by reaction of $[Cp^*Ir(OH_2)_3][SO_4]$ with bipyridine derivatives and crystals grown from the aqueous mother liquors. This different procedure may explain the variation in the molecular structures obtained in the solid state.

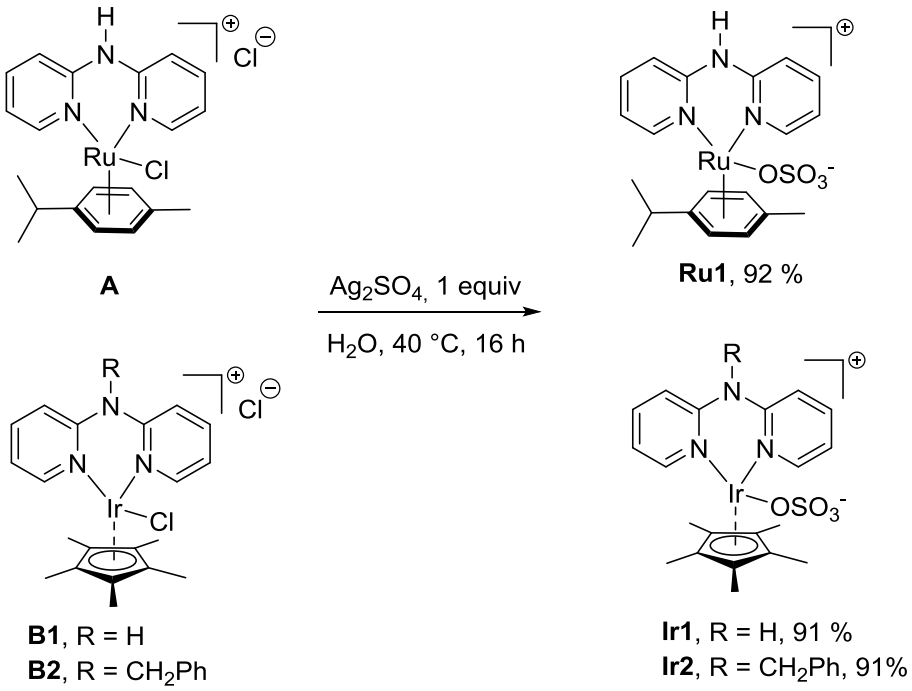

Scheme 1 Synthesis of new complexes Ru1, Ir1 and Ir2

Since the nature of the crystallization solvents may have an influence on the coordination sphere of these complexes particularly with MeOH which lead to H-bonding with coordinated [OSO_3] (Figure 1a), we crystallized the same complex in a mixture of CH_2Cl_2/Et_2O. Despite this solvent change the nature of the complex remained zwitterionic. In this case, intermolecular H-bonding between coordinated [OSO_3] and N-H was evidenced in the molecular structure (Figure 1b). **Ir2** and **Ru1** also featured a zwitterionic molecular structure as depicted in Figure 1c and 1d, respectively. Unfortunately, we did not succeed to grow crystals of **Ir1** or **Ir2** in water.

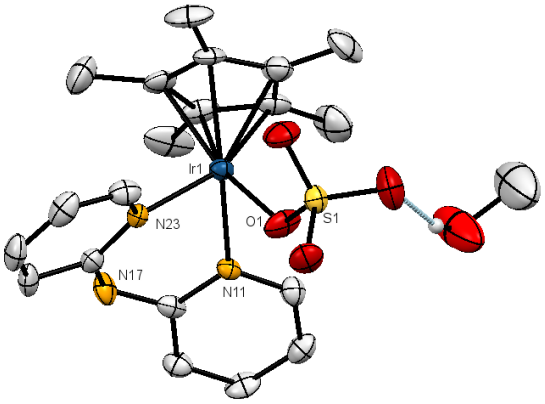

(a)
Selected bond lengths (Å) and angles (°): Ir1-N11: 2.104; Ir1-N23: 2.096; Ir1-O1: 2.101: Ir1-Cp*centroid: 1.786; N11Ir1N23: 84.06; N23Ir1O1: 82.73: O1Ir1N11: 79.63

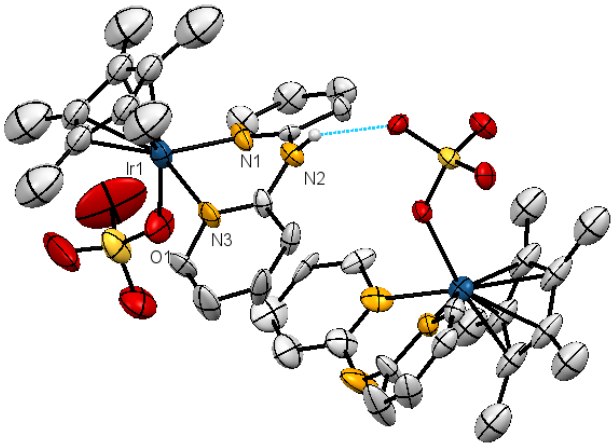

(b)
Selected bond lengths (Å) and angles (°): Ir1-N1: 2.077; Ir1-N3: 2.091; Ir1-O1: 2.089: Ir1-Cp*centroid: 1.821; N3Ir1N1: 83.83; N1Ir1O1: 83.05: O1Ir1N3: 80.01

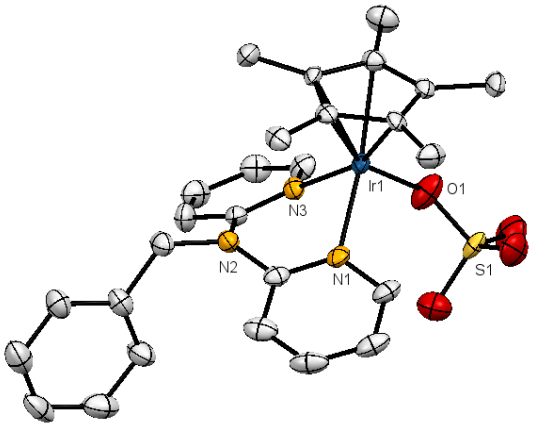

(c)
Selected bond lengths (Å) and angles (°): Ir1-N3: 2.076; Ir1-N1: 2.094; Ir1-O1: 2.120: Ir1-Cp*centroid: 1.769; N3Ir1N1: 81.96; N1Ir1O1: 97.33: O1Ir1N3: 81.88

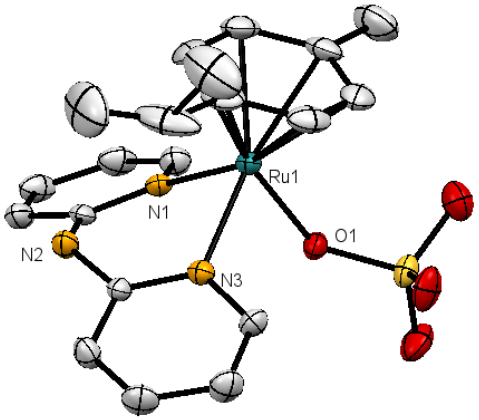

(d)
Selected bond lengths (Å) and angles (°): Ru1-N1: 2.085; Ru1-N3: 2.097; Ru1-O1: 2.095: Ir1-*p*-cymene centroid: 1.683; N1Ru1N3: 83.64; O1Ru1N1: 81.07: N3Ru1O1: 83.71

Figure 1 Molecular structure of **Ir1** (a) crystallised in MeOH/ Et_2O, (b) crystallised in CH_2Cl_2/Et_2O. **Ir2** (c). **Ru1** (d). Solvent and H are omitted except to highlight H-bonding in (a) and (b)

For better understanding the origin of these different solid state molecular structures, the synthesis of the [Cp*(bpy)Ir][SO4] complex was performed as described in the literature

(Scheme 2) and crystals were grown in a CH_2Cl_2/Et_2O mixture instead of water. Using this procedure, the complex crystallised in a zwitterionic structure with a sulfato-ligand displaying H-bonding with a water molecule (Figure 2) demonstrating that these solid state structure are highly dependent upon the crystallization solvents used.[16] However, it is very likely that these complexes are present as ion pairs when dissolved in water.

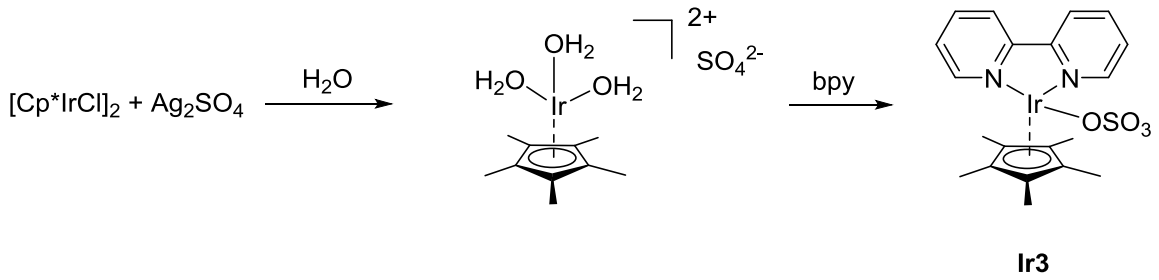

Scheme 2 Synthesis of **Ir3** [Cp*Ir(bpy)(OSO3)] complex

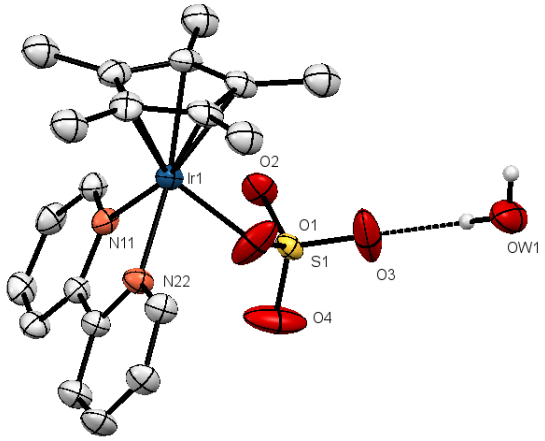

Figure 2 Molecular structure of **Ir3** [Cp*Ir(bpy)OSO_3]. H atom omitted except in the H-bonded water molecule. Selected bond lengths (Å) and angles (°): Ir1-N11: 2.094; Ir1-N22: 2.091; Ir1-O1: 2.080, Ir1-Cp* centroid: 1.783; N11Ir1N22: 77.07; N11Ir1O1: 86.17; N22Ir1O1: 79.68

Catalysis

Transfer hydrogenation

The three new complexes **Ru1**, **Ir1** and **Ir2** were evaluated in the reduction of levulinic acid into γ-valerolactone. In the literature, transfer hydrogenation and hydrogenation processes are most often opposed. Transfer hydrogenation is rightly considered as a safer transformation than hydrogenation, this latter being however a more atom-efficient reaction.

In order to get a full overview of the potential of our new catalysts we investigated their efficiency in both base free transfer hydrogenation and hydrogenation.

The transfer hydrogenation of LA was first investigated under various conditions of temperature, catalyst loading and solvents (Scheme 3).

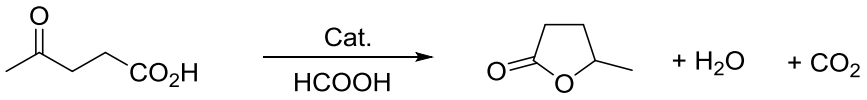

Scheme 3 Transfer hydrogenation of LA

As depicted in Table 1, iridium-based catalysts were active under base free conditions, as expected from removal of the chloride ligand in these complexes as compared to **B1** and **B2**. A preliminary screening under neat conditions revealed the best performances obtained with **Ir1** vs **Ir2** whereas **Ru1** was inactive under similar conditions (Table 1, entries 1-6). **Ir1** was thus selected for further studies in water where best performances were obtained at 110 °C with a 1 M and 0.5 M concentration of levulinic acid (Table 1, entries 7-10). The catalyst loading could be further decreased to 0.01 mol% but the reaction required longer reaction time to reach full conversion and high yield of γ-valerolactone (Table 1, entry 13). Under these conditions a TON of 9000 was reached which is close to the highest TON reported thus far for the transfer hydrogenation of LA (9800)[9]. Further attempts to increase the reaction productivity were not successful (Table 1, entries 14-15). No conversion was observed using isopropanol instead of formic acid as hydrogen donor with all three catalysts (0.05 mol% catalysts, 110 °C, 16 h, *i*PrOH (2 mL))

Table 1 Transfer hydrogenation of levulinic acid[a]

Entry	Cat (mol%)	t (h)	T °(C)	Solvent	Conv (%)[b]
1	**Ru1** (0.1)	16	110	neat	< 2
2	**Ir1** (0.1)	16	110	neat	73
3	**Ir2** (0.1)	16	110	neat	57
4	**Ir1** (0.1)	16	120	neat	73
5	**Ir1** (0.1)	16	140	neat	85 (83)
6[c]	**Ir1** (0.1)	16	120	neat	70
7	**Ir1** (0.1)	16	110	H_2O, [LA] = 2 mol.L^{-1}	70
8	**Ir1** (0.1)	16	110	H_2O, [LA] = 1 mol.L^{-1}	100 (99)
9	**Ir1** (0.1)	16	110	H_2O, [LA] = 0.5 mol.L^{-1}	100
10	**Ir1** (0.1)	16	110	H_2O, [LA] = 0.33 mol.L^{-1}	77
11	**Ir1** (0.05)	16	110	H_2O, [LA] = 1 mol.L^{-1}	77
12	**Ir1** (0.05)	24	110	H_2O, [LA] = 1 mol.L^{-1}	100 (99)
13	**Ir1** (0.01)	72	110	H_2O, [LA] = 1 mol.L^{-1}	92 (90)
14	**Ir1** (0.001)	16	110	H_2O, [LA] = 1 mol.L^{-1}	< 2
15	**Ir1** (0.001)	16	130	H_2O, [LA] = 1 mol.L^{-1}	< 2

[a] LA (0.232 g, 2 mmol), FA (0.184 g, 4 mmol)

[b] Determined by ^1H NMR (isolated yield)

[c] with 1 equiv. of Et_3N

In 2009, Fu and Guo observed a rapid increase of pressure in a reactor where a ruthenium-catalyzed transfer hydrogenation of LA was supposed to take place.[10b] They postulated the fast dehydrogenation of formic acid into H_2 and CO_2 and concluded that GVL was obtained by

hydrogenation of LA rather than transfer hydrogenation. The possible contribution of hydrogenation during the transfer hydrogenation of LA catalysed by **Ir1** was considered since this catalyst may also be an efficient FA dehydrogenation catalyst as many cationic Cp*Ir(bipyridine) and related complexes.[17] In order to fully address this issue, a series of experiments was conducted having in mind that the potential hydrogenation of LA during a transfer hydrogenation experiment cannot be strictly compared to a hydrogenation reaction due to different metal-hydride formation pathways at the onset of the reaction. As opposed to conventional hydrogenation requiring activation of H_2 into M-H or M(H_2), hydrogenation occurring in a transfer reaction process with formic acid will be initiated by the formation of M-H from formic acid dehydrogenation. **Ir1** was first evaluated in the dehydrogenation of FA under experimental conditions identical to those used for TH of levulinic acid (FA, 4 mmol; **Ir1**, 0.05 mol% vs FA, 110 °C) using an eudiometer system to measure the volume of released gas. **Ir1** was indeed found to be an efficient formic acid dehydrogenation catalyst leading to complete dehydrogenation of FA in 1 h (see SI, p S9, Figure S2). The dehydrogenation was also measured under GVL synthesis conditions (LA, 2 mmol; FA, 4 mmol; **Ir1**, 0.1 mol% vs LA, 110 °C) where it was found that the dehydrogenation rate was slower and complete dehydrogenation was not reached after 2 h (see SI, p S9). In this experiment GVL was obtained in 30% yield (^{1}H NMR) thus accounting for the lower gas volume released due to FA consumption in the transfer hydrogenation of LA. This result was confirmed by implementing the transfer hydrogenation of LA at 110 °C in an open system yielding GVL in 30-35 % yield. These results demonstrate that transfer hydrogenation is operative for the transformation of LA into GVL in an open system, despite formic acid dehydrogenation. The situation is somewhat different in a closed system considering the 2 reaction pathways depicted in Figure 3 (**A** for transfer hydrogenation and **B**+**D**

for hydrogenation). Two parameters should be here carefully considered. First, the pressure generated during this reaction reached ~ 5 bar. Since pathway **A** also generates CO_2, the partial pressure of H_2 can be estimated below 2.5 bar. However, as it will be reported in the next paragraph, this pressure is high enough, albeit not optimum, for the hydrogenation of LA. The reversibility of formic acid dehydrogenation (Figure 3, pathway **C**) should also be considered owing to the concomitant consumption of formic acid and CO_2 release in pathway **A**. However, hydrogenation of CO_2 usually requires high pressure and more importantly basic conditions to overcome unfavourable thermodynamic properties,[18] this process is therefore unlikely under acidic conditions and a total pressure reaching a maximum of 5 bar.[19] In order to fully address this issue, a series of experiments was conducted using two Schlenk tubes connected by a glass tube (see SI, p S6). In a first experiment one Schlenk tube was filled with formic acid, **Ir1** (0.05 mol%) and water (2 mL) and the second Schlenk tube was filled with levulinic acid, **Ir1** (0.1 mol%) and water (2 mL). These two Schlenk tube were heated at 110 °C for 16 h. Only 13% yield of GVL was obtained in the second flask. An almost identical experiment was repeated with addition of a catalytic amount of formic acid in the second Schlenk tube in order to mimic more closely the experimental conditions implemented in transfer hydrogenation experiments, in particular concerning formation of the Ir-H species. When 1 equiv. and 10 equiv. of formic acid with respect to **Ir1** were used, the yield of GVL increased to 19% and 65%, respectively hence confirming that hydrogenation of LA benefits from the easier formation of the same metal-hydride species arising from iridium formate. All together, these results demonstrate that transfer hydrogenation of levulinic acid into GVL in a closed system operates essentially by hydrogenation rather than transfer hydrogenation.

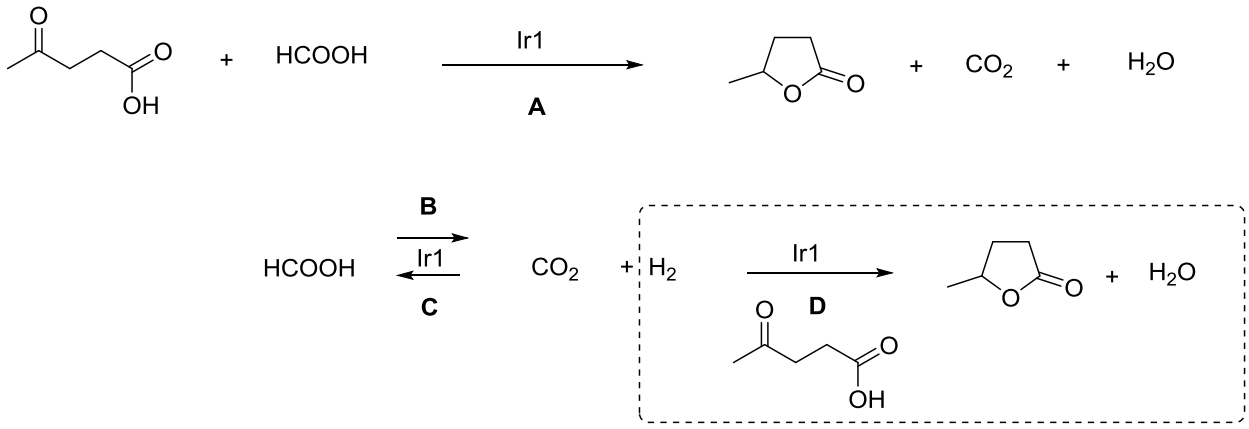

Figure 3 Synthesis of GVL under transfer hydrogenation conditions

Hydrogenation

In a second set of experiments, catalysts were evaluated under base free hydrogenation conditions (Scheme 4, Table 2)

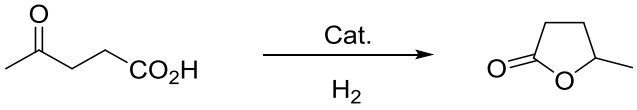

Scheme 4 Hydrogenation of LA

The influence of the H_2 pressure was first investigated at 130 °C in water. We were pleased to observe that **Ir1** could operate under 5 bar of H_2 (Table 2, entries 1-4). As observed under transfer hydrogenation conditions, **Ru1** was found to be less efficient than **Ir1** at 130 °C, this difference being more important upon lowering the reaction temperature to 110 °C (Table 2 entries 4,5 and 6,7). Improvement of the catalyst productivity was then attempted by lowering the catalyst loading to 0.05 mol%. With this low catalyst loading the conversion of LA remained almost quantitative with **Ir1** while it was only 30 % with **Ir2** (Table 2, entries 10,11). Further

decrease of the catalyst loading required prolonged reaction time to reach full conversion hence demonstrating the high stability of the catalyst (Table 2, entries 12,13). Further decrease in catalyst loading led to a TON of 97000 obtained in 36 h at 110 °C (Table 2, entry 16) and the reaction could be scaled up to 1 g without loss of yield (Table 2, entry 17). Finally, the TON could be further increased to 174000 at 130 °C (Table 2, entry 18). To the best of our knowledge, this is the highest TON reported so far for this base-free transformation.

Table 2 Hydrogenation of levulinic acid[a]

Entry	Cat (mol%)	t (h)	T °(C)	P H_2 (bar)	Solvent	Conv (%)[b]
1	**Ir1** (0.1)	16	130	40	H_2O, [LA] = 4 mol.L^{-1}	94
2	**Ir1** (0.1)	16	130	40	H_2O, [LA] = 2 mol.L^{-1}	100
3	**Ir1** (0.1)	16	130	40	H_2O, [LA] = 1 mol.L^{-1}	100
4	**Ir1** (0.1)	16	130	5	H_2O, [LA] = 1 mol.L^{-1}	100
5	**Ru1** (0.1)	16	130	5	H_2O, [LA] = 2 mol.L^{-1}	92 (90)
6	**Ir1** (0.1)	16	110	5	H_2O, [LA] = 2 mol.L^{-1}	100
7	**Ru1** (0.1)	16	110	5	H_2O, [LA] = 2 mol.L^{-1}	13
8	**Ir1** (0.1)	16	110	2	H_2O, [LA] = 2 mol.L^{-1}	90
9	**Ir1** (0.05)	12	110	5	H_2O, [LA] = 2 mol.L^{-1}	87 (85)
10	**Ir1** (0.05)	16	110	5	H_2O, [LA] = 2 mol.L^{-1}	100 (99)
11	**Ir2** (0.05)	16	110	5	H_2O, [LA] = 2 mol.L^{-1}	30
12	**Ir1** (0.01)	16	110	5	H_2O, [LA] = 2 mol.L^{-1}	27
13	**Ir1** (0.01)	72	110	5	H_2O, [LA] = 2 mol.L^{-1}	100 (99)
14	**Ir1** (0.001)	16	110	5	H_2O, [LA] = 2 mol.L^{-1}	10
15	**Ir1** (0.001)	16	130	5	H_2O, [LA] = 2 mol.L^{-1}	66
16	**Ir1** (0.001)	32	130	5	H_2O, [LA] = 2 mol.L^{-1}	98(97)
17[d]	**Ir1** (0.001)	32	130	5	H_2O, [LA] = 2 mol.L^{-1}	96 (95)
18	**Ir1** (0.0005)	72	130	5	H_2O, [LA] = 2 mol.L^{-1}	87 (87)[c]

[a] LA (0.232 g, 2 mmol)

[b] Determined by ^1H NMR (isolated yield)

[c] This reaction was checked two times furnishing GVL in 92% and 83% NMR yield.

[d] LA (1.16 g, 10 mmol)

The interest of a catalytic system does not only rely on its efficiency but also on its ability to be used in a continuous process or reused in recycling experiments. The recyclability of **Ir1** was thus evaluated with a low initial catalyst loading and shortest reaction time[20] (Table 2, entries 15 &16). With these conditions, **Ir1** could be reused 3 times without significant decrease of efficiency thus highlighting again its high stability (Table 3). **Ir1** thus displays high activity and stability that could be later valorized in continuous processes.

Table 3 Ir1 recycling for hydrogenation of LA [a]

Run	GVL yield (%)[b]
1	97
2	97
3	95

[a] LA (0.232 g, 2 mmol), **Ir1** (0.001 mol%), H_2O (2 mL), P(H_2) = 5 bar, 110 °C, 32 h.

[b] determined by NMR

As mentioned in the introduction, levulinic acid can be obtained by acidic treatment of various carbohydrates with concomitant formation of formic acid. It is thus possible to generate GVL directly from this reaction mixture by adding a hydrogenation or transfer hydrogenation catalyst. This process has been extensively studied with heterogeneous catalysts[4] but only few reports deal with homogeneous catalyst.[9,10b,d] To highlight the potential of **Ir1**, we attempted the synthesis of GVL directly from carbohydrates (glucose and fructose) by means of transfer hydrogenation and hydrogenation. Carbohydrates were first dehydrated by acidic treatment at 180 °C (Scheme 5). The reaction mixture was filtrated to remove insoluble materials before

addition of **Ir1**. The reactor was then pressurized with 5 bar of hydrogen and heated at 130 °C for 32 h. Under these conditions, both glucose and fructose led to GVL in 57% and 53% isolated overall yield, respectively. These moderate yields are in the range of those observed using homogeneous[9, 10b, 10d,] or heterogeneous catalysts.[21] These moderate yields can be explained by an incomplete conversion of levulinic acid (85 %) but also by formation of insoluble materials (humins) observed during the first step of the reaction.[22] More interestingly, GVL was also synthesized with formic acid generated during acidic hydrolysis of glucose serving as the sole hydrogen source. Under these conditions GVL was isolated in 44% yield.

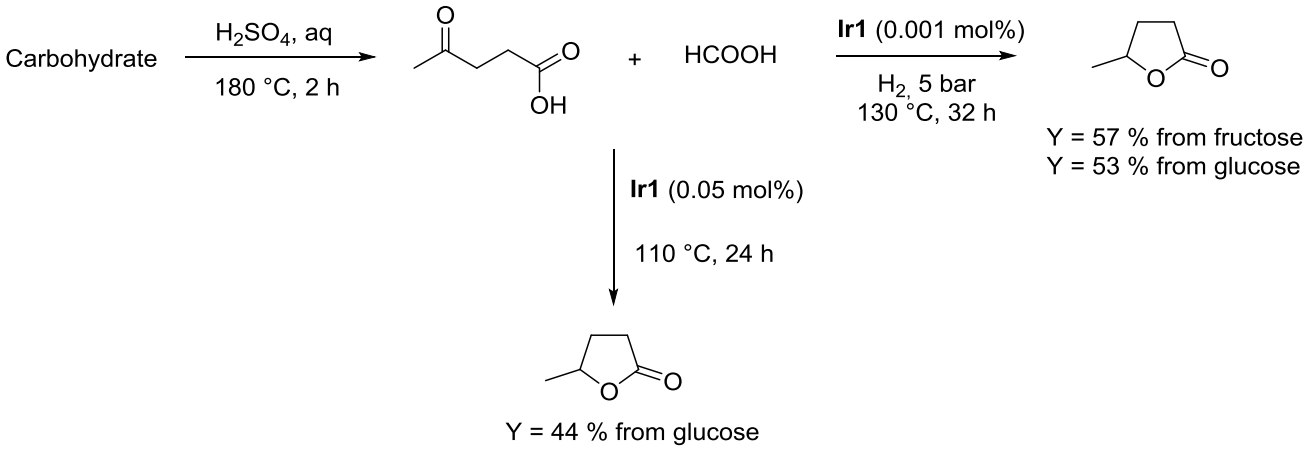

Scheme 5 Direct synthesis of GVL from carbohydrates

Following these studies, we turned our attention to the influence of the counter anion and prepared a series of complexes containing non-coordinating PF_6 anions. These complexes were prepared in good yields from **Ru1**, **Ir1**, **Ir2**, by anion metathesis with KPF_6 (Scheme 1) and fully characterized by NMR, HRMS and by X-Ray except fot **Ir2'** for which we did not succeed to grow crystals of sufficient quality (see SI).

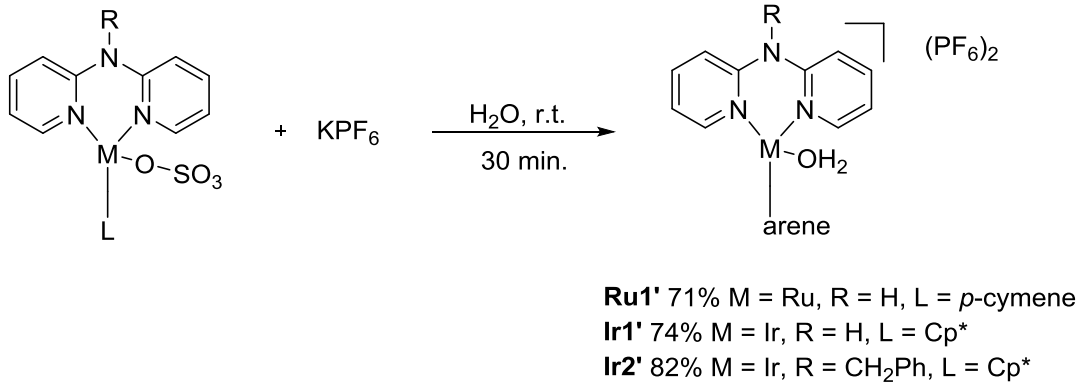

Scheme 6 Synthesis of **Ru1'**, **Ir1'**, **Ir2'**

These complexes were evaluated in the reduction of LA into GVL using HCOOH or H_2. As depicted in Table 4, these new complexes were slightly less efficient than their sulphonate counterparts. Of note, **Ru1'** was still poorly reactive hence minimizing a possible poisoning by the coordinating sulfate anion in **Ru1**. In addition, as observed with the three sulphonate complexes, transfer hydrogenation in isopropanol (without formic acid) did not provide any conversion of LA.

Table 4 Transfer hydrogenation and hydrogenation of levulinic acid with **Ru1'**, **Ir1'**, **Ir2'**[a]

Entry	Cat (mol%)	FA (equiv.)	P H_2 (bar)	Conv (%)[b]
1	**Ru1**' (0.05)	2	-	0
2	**Ir1**' (0.05)	2	-	66 (100% with **Ir1**)
3	**Ir2'** (0.05)	2	-	32
4	**Ru1**'(0.05)	-	5	8 (13% with 0.1 mol% **Ru1**)
5	**Ir1**' (0.05)	-	5	85 (100% with **Ir1**)
6	**Ir2'** (0.05)	-	5	35 (30% with **Ir2**)

[a] LA (0.232 g, 2 mmol), H_2O (2 mL), 110 °C, 16 h.

[b] Determined by ^1H NMR (isolated yield)

In order to prove the general applicability of **Ir1**, we have extended the scope of the reaction to other substrates and reactions. As displayed in Scheme 7, **Ir1** was efficient for the reductive cyclisation of 2-formylbenzoic acid (a), the reduction of acetophenone (b) and for the synthesis of a six-membered lactone (c).

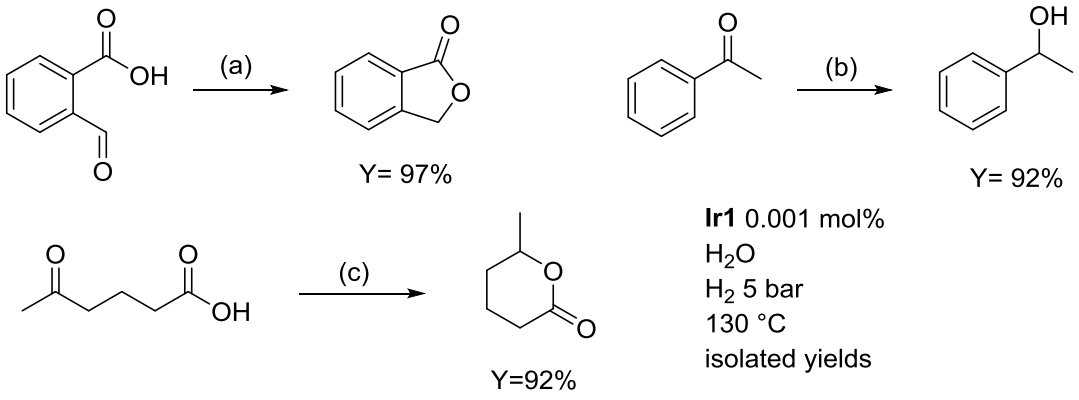

Scheme 7 Scope of products accessible with **Ir1** catalyst

Mechanism studies

Having demonstrated the much better performances obtained in hydrogenation vs transfer hydrogenation we focused our investigations on the hydrogenation process with **Ir1**. We first looked at the nature of the iridium species generated by reaction of **Ir1** with hydrogen. A pressure NMR tube was loaded with **Ir1** dissolved in DMSO-d6 and the tube was pressurized with 1.5 bar of H_2 (Scheme 8).

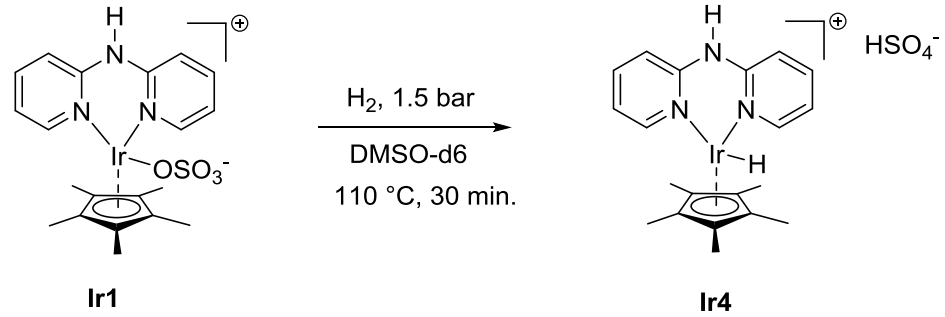

Scheme 8 Synthesis of Ir-hydride complex **Ir4**

After 30 minutes at 110 °C, ^{1}H NMR was monitored covering a broad window of possible Ir-H chemical shifts (see SI, Figure S14, p S17). As depicted in Figure 4, a very clean NMR spectra was obtained with a singlet at -9.37 ppm integrating for 1 H hence demonstrating the presence of an Ir-H complex without trace of iridium dihydride species. Unfortunately, it was not possible to grow crystals of this **Ir4** compound. Other methods employing $NaBH_4$ or formic acid failed to furnish this Ir-H complex. This problem in obtaining a molecular structure of the iridium hydride complex prompted us to turn our attention to a parent complex with a non-coordinating PF_6 anion.

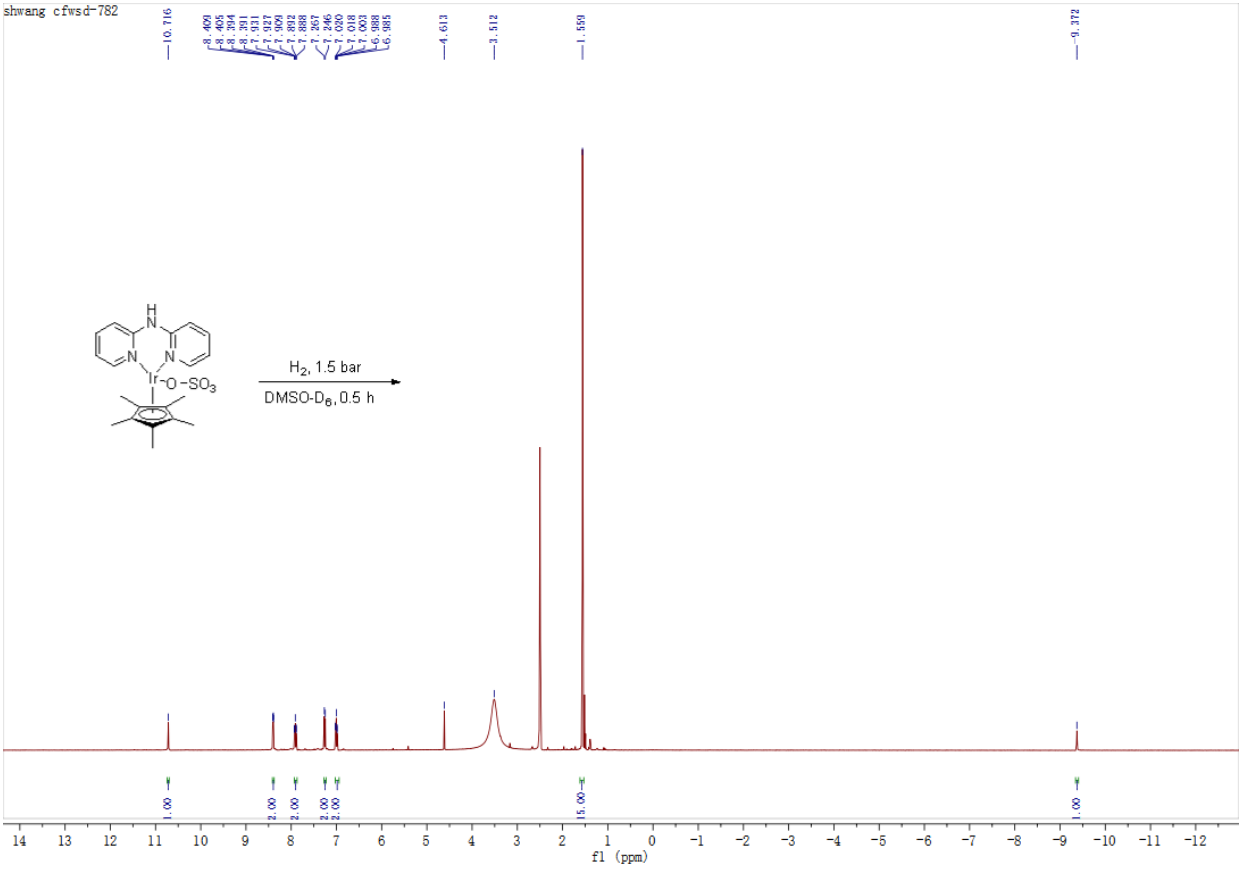

Figure 4 ^{1}H NMR of the iridium hydride complex **Ir4**

This complex **Ir5** was best prepared by reacting **Ir1** with HCOONa followed by anion metathesis with KPF_6 (Scheme 9). The NMR of this complex was very similar to that of **Ir4**, in particular a singlet centered at -9.43 ppm integrating for 1 H was also detected (see SI, p S18). This complex could be isolated and suitable crystals were obtained for molecular structure determination (Figure 5). With this complex in hands, we evaluated its catalytic activity in the transfer hydrogenation and hydrogenation of LA. As depicted in Scheme 9, **Ir5** led to quantitative yields of GVL in both processes hence confirming the probable intermediacy of such iridium hydride complex in the transformations catalyzed by **Ir1**. **Ir5** was also evaluated under transfer hydrogenation of LA with low catalyst loading (0.05 mol%). In that case, full conversion was obtained when only 77% conversion was reached with the in situ generated catalyst (Table 1, entry 11). This result can be explained by the incomplete transformation of **Ir1** into active Ir-H species when in situ generated.

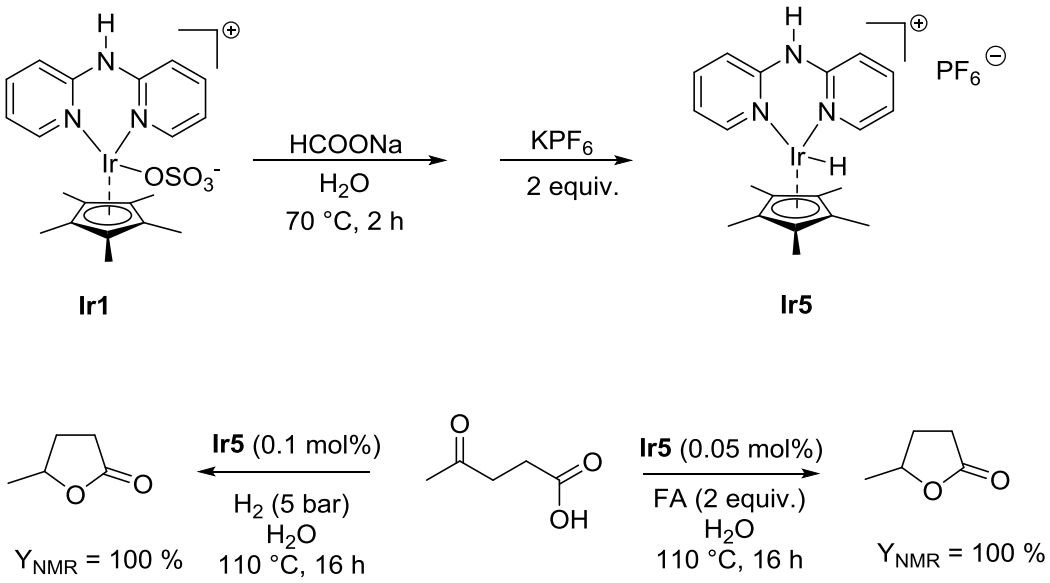

Scheme 9 Synthesis and catalytic performances of iridium hydride complex **Ir5**

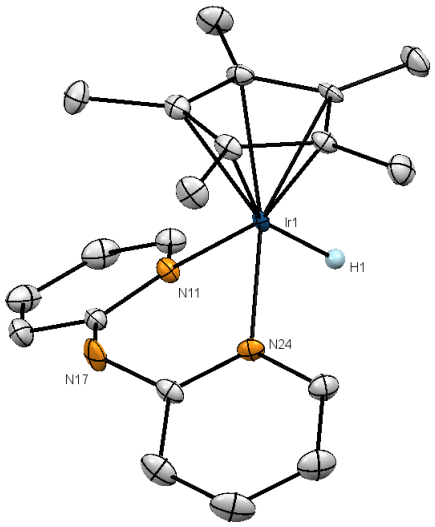

Figure 5 Molecular structure of **Ir5**. PF_6 anion and H atoms are omitted for clarity excepted Ir-H Selected bond lengths (Å) and angles (°): Ir1-N11: 2.098; Ir1-N24: 2.086; Ir1-Cp*centroid: 1.825; Ir1-H1: 1.825; N11Ir1N24: 84.32: N11Ir1H1: 86.92; N24Ir1H1: 88.83.

Based on these results a reaction mechanism is proposed in Figure 6. η^2-H_2 complexes are commonly considered as the starting intermediate in hydrogenation reaction. These compound can evolve by homolytic cleavage of H_2 leading to a dihydride complex or by heterolytic cleavage of H_2 assisted by a base leading to a monohydride complex.[23] Characterisation of monohydride species **Ir4** and **Ir5** is consistent with the latter mechanism. η^2-H_2 complexes are in general acidic compounds with some negative reported pKa[24] which may explain in our case the deprotonation of **A** by a weak base such as SO_4^{2-} leading to the monohydride iridium complex **B**. An alternative pathway would involve a sigma-bond metathesis with a coordinated water molecule leading to **A'**.[25] This pathway, does not involve a base (other than H_2O) and could better account for the catalysis with non-coordinating and non-basic PF_6 complexes. Further hydride transfer to LA (**C**) generates the alkoxo-iridium complex **D**. It is generally reported that 4-hydroxyvaleric acid (**4-HVA**) is produced upon protonation of iridium-alcoxo species **D** and a

further intramolecular transesterification would generate GVL. However, it is barely impossible to find any observation on the presence of **4-HVA** in reaction mixtures in articles dealing with the synthesis of GVL from LA. A very interesting IR and ^{1}H NMR in situ monitoring by Mika did not mention the detection of **4-HVA**.[26] The same observation was clearly stated more recently by Makhubela and Darkwa.[27] In our case, we could not detect any trace of **4-HVA** in any of our multiple experiments. All these elements are consistent with an alternative pathway operating without release of **4-HVA**. We suggest that an intramolecular metal-assisted cyclization may occur from species **D** likely involving activation of the carboxylic function by the iridium centre. Several options regenerating dicationic or monocationic iridium complexes would then be possible to close the catalytic cycle (dashed arrows)

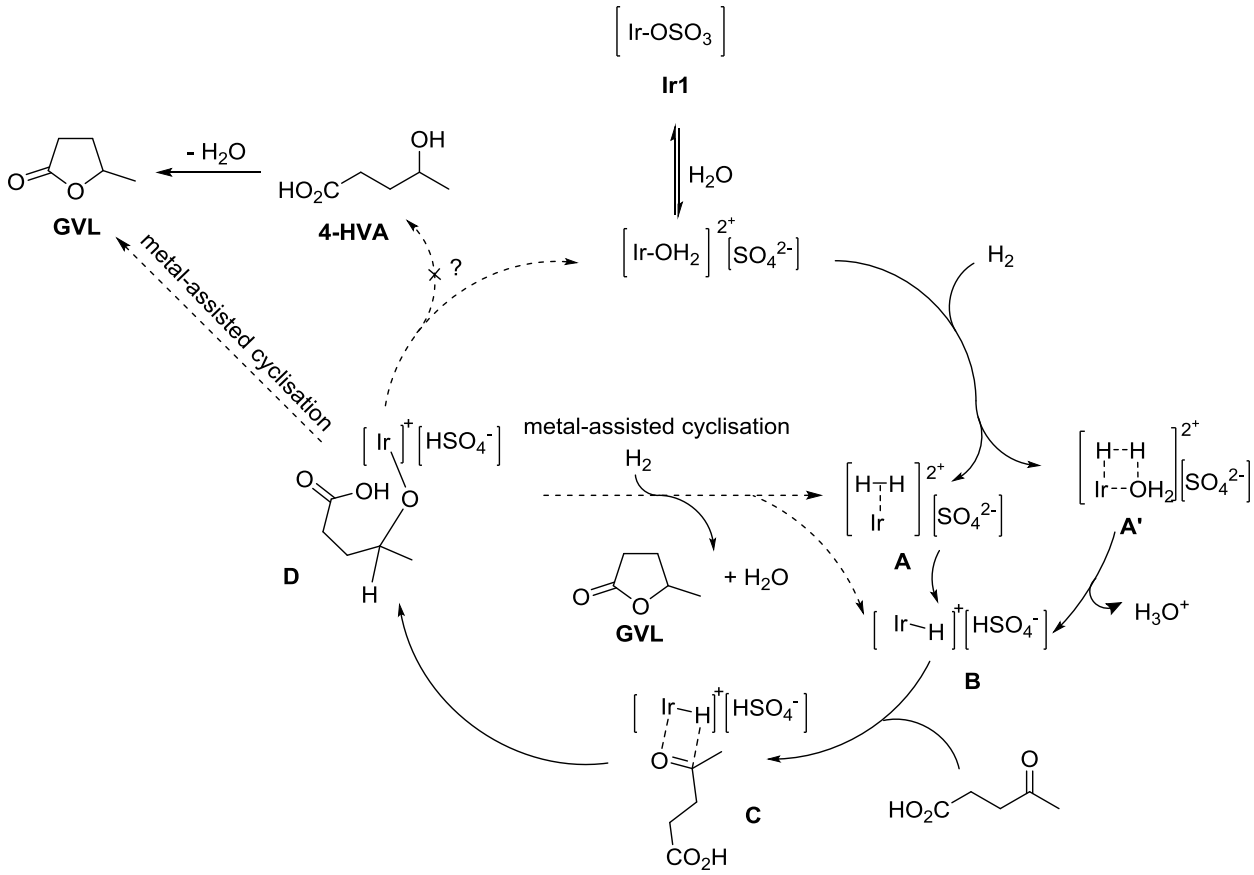

Figure 6 Postulated mechanism for the **Ir1**-catalyzed hydrogenation of LA

CONCLUSION

We have prepared and characterized 7 new complexes of which [Cp*Ir(dpa)(OSO_3)] **Ir1** was found very efficient in transfer hydrogenation and hydrogenation of levulinic acid. Of note, this catalyst reached the highest TONs reported to date both in transfer hydrogenation and hydrogenation of levulinic acid. However, we have demonstrated that under transfer hydrogenation conditions, the reaction does essentially proceed by hydrogenation involving formic acid dehydrogenation as suggested by Guo in 2009. For this reason, the potential of **Ir1** in formic acid dehydrogenation is currently being investigated in our group. The full potential of **Ir1** was also highlighted by its high stability enabling efficient recycling in hydrogenation of LA and by a the 2-step synthesis of GVL from carbohydrates. Finally, based on the characterization of an Ir-H complex intermediate under hydrogen gas pressure and the isolation of **Ir5**, we propose a mechanism that involves heterolytic H2 splitting from Ir(η^2-H2). The ring closing step occurs without the intermediacy of 4-hydroxyvaleric acid, which could not be observed under a variety of conditions. The high performances of this catalyst in the reduction of LA open the way for its utilization in other types of reduction transformations of bio-sourced compounds that are currently under investigation in our group.

EXPERIMENTAL SECTION

General Information:

Levulinic acid (98%), formic acid (98%), silver sulfate (99.999%), fructose (99%), glucose (99%), 2,2'-dipyridylamine (98%) and acetophenone (99%) were purchased from Sigma-Aldrich. H_2 Alphagaz grade ($H_2O \leq 3$ ppm; $O_2 \leq 2$ ppm) was purchased from Air Liquide. Solvents (methanol, diethyl ether, water, dichloromethane) were HPLC grade and used as

received. [(dpa)(*p*-cymene)RuCl]Cl, [(dpa)Cp*IrCl]Cl and [(bdpa)Cp*IrCl]Cl were synthesized as described in the literature.[12b] ^{1}H NMR spectra were recorded on a Bruker Avance (400 MHz) spectrometer and reported in ppm with reference to H_2O (4.79 ppm), DMSO (2.5 ppm). Data are reported as follows: s= singlet, d= doublet, t= triplet, q= quartet, m= multiplet. Coupling constants are reported in Hz. ^{13}C NMR spectra were recorded at 100 MHz on the same spectrometer and reported in ppm with reference to DMSO (39.5 ppm).

Synthesis of organometallic complexes

- Synthesis of [(dpa)(*p*-cymene)RuOSO$_3$] **Ru1**:

[(dpa)(*p*-cymene)RuCl]Cl (0.047 g, 0.1 mmol) was weighed into a 20 mL Schlenk tube and dissolved in 2 ml of water. Silver sulfate (0.031 g, 0.1 mmol) was added and the reaction mixture was stirred at 40 ^{o}C for 16 h. The suspension was filtered by cannula into a clean Schlenk tube. The solvent was removed under vacuum and the resulting solid was washed with diethyl ether (3 x 5 ml), then dried overnight under vacuum to give 0.046 g (yield: 92%) of the desired product as a yellow solid. ^{1}H NMR (400 Hz, D_2O): δ 8.71 (d, $^{3}J_{H-H}$ = 5.6 Hz, 2H, CH), 8.02-7.98 (m, 2H, CH), 7.33-7.29 (m, 4H, CH), 5.89 (d, $^{3}J_{H-H}$ = 8.4 Hz, 2H, *p*-cymene CH), 5.80 (d, $^{3}J_{H-H}$ = 8.4 Hz, 2H, *p*-cymene CH), 2.54 (hept, $^{3}J_{H-H}$ = 6.8 Hz,1H, iPr CH), 2.10 (s, 3H, CH_3), 1.18 (d, $^{3}J_{H-H}$ = 6.8 Hz, 6H, iPr CH_3); ^{13}C {^{1}H} NMR (100 MHz, D_2O): δ 152.6, 152.3, 141.4, 120.0, 114.9, 104.5, 100.2, 84.2, 83.7, 30.4, 21.1, 17.1.

HRMS (ESI, H_2O): m/z calculated for $C_{20}H_{23}N_3O_4NaSRu$: 526.0350; m/z measured: 526.0349

- Synthesis of [(dpa)Cp*IrOSO$_3$] **Ir1**:

[(dpa)Cp*IrCl]Cl (0.057 g, 0.1 mmol) was weighed into a 20 mL Schlenk tube and dissolved in 2 ml of water. Silver sulfate (0.031 g, 0.1 mmol) was added and the reaction mixture was stirred at 40 ^{o}C for 16 h. The suspension was filtered into a clean Schlenk tube. The solvent was

removed under vacuum and the resulting solid was washed with diethyl ether (3 x 5 ml) and dried overnight under vacuum to give 0.054 g (yield: 91%) product as yellow solid.

^{1}H NMR (400 Hz, D_2O): δ 8.46 (d, $^{3}J_{H-H}$ = 5.6 Hz, 2H, CH), 8.02 (m, 2H, CH), 7.43 (d, $^{3}J_{H-H}$ = 8.4 Hz, 2H, CH), 7.34 (m, 2H, CH), 1.47 (s, 15H, Cp* CH_3); ^{13}C {^{1}H} NMR (100 MHz, D_2O): δ 151.0, 150.4, 141.9, 121.4, 115.2, 88.1, 7.7.

HRMS (ESI, H_2O): Dicationic compound detected as the major product m/z (z = 2) calculated for $C_{20}H_{24}N_3Ir$: 249.5794; m/z measured: 249.5797

- Synthesis of (bdpa)Cp*IrO_4S **Ir2**:

With the same procedure as for the synthesis of **Ir1**, **Ir2** was obtained as a yellow powder (yield: 91%).^{1}H NMR (400 MHz, D_2O) δ 8.61-8.60 (m, 2H, CH), 7.98-7.93 (m, 2H), 7.53-7.37 (m, 9H, CH), 5.54 (s, 2H, CH_2), 1.49 (s, 15H, Cp* CH_3); ^{13}C NMR (100 MHz, D_2O) δ 153.8, 151.0, 142.3, 134.2, 129.0, 128.0, 126.6, 122.5, 116.8, 88.3, 56.2, 7.6.

HRMS (ESI, H_2O): m/z Calculated for $C_{27}H_{30}N_3O_4NaSIr$: 708.1484; m/z measured: 708.1481

- Synthesis of [Cp*Ir(bpy)OSO_3] **Ir3**:

[Cp*$IrCl_2$]$_2$ (0.079 g, 0.1 mmol) and silver sulfate (0.062 g, 0.2 mmol) were added in water (2 ml), and the reaction mixture was stirred at r.t. for 16 h. The suspension was filtered by cannula into a clean Schlenk tube and bipyridine (0.031 g, 0.2 mmol) was added. The mixture was stirred at 40 ^{o}C for 16 h. Then the solvent was removed under vacuum and the resulting solid was washed with diethyl ether (3 x 5 ml), then dried overnight under vacuum to give 0.043g (yield: 74%) of the desired product obtained as a yellow solid. ^{1}H NMR (400 Hz, D_2O): δ 9.15 (d, $^{3}J_{H-H}$= 5.2 Hz, 2H, CH), 8.57 (d, $^{3}J_{H-H}$= 8.4 Hz, 2H, CH), 8.36 (dd, $^{3}J_{H-H}$= 8.0 Hz, 2H, CH), 7.92 (dd,

$^{3}J_{H-H}$ = 6.0 Hz, 2H, CH), 1.69 (s, 15H, Cp* CH_3); $^{13}C\{^{1}H\}$ NMR (100 MHz, D_2O): δ156.0, 151.6, 141.6, 129.3, 124.3, 89.3, 7.7.

HRMS (ESI, H_2O): m/z Calculated for $C_{20}H_{23}N_2Ir^{2+}$: 242.0739; m/z measured: 247.0742

- Synthesis of [(dpa)(*p*-cymene)Ru]$(PF_6)_2$ **Ru1'**:

[(dpa)(*p*-cymene)$RuOSO_3$] (0.050 g, 0.1 mmol) was weighed into a 20 mL Schlenk tube and dissolved in 2 ml of water. Potassium hexafluorophosphate (0.040 g, 0.22 mmol, 2.2 eq) was added and the reaction mixture was stirred at room temperature for 30 min. The suspension was filtered by cannula. The resulting solid was washed with cooled water (1 ml), then dried overnight under vacuum to give 0.051 g (yield: 71%) of the desired product obtained as a brown solid. ^{1}H NMR (400 Hz, D_2O): δ 8.70 (d, $^{3}J_{H-H}$= 5.6Hz, 2H, CH), 8.02-7.98 (m, 2H, CH), 7.33-7.28 (m, 4H, CH), 5.88 (d, $^{3}J_{H-H}$ = 6.4 Hz, 2H, *p*-cymene CH), 5.79 (d,$^{3}J_{H-H}$= 6.0 Hz, 2H, *p*-cymene CH), 2.54 (hept, $^{3}J_{H-H}$ = 6.8 Hz,1H, iPr CH), 2.10 (s, 3H, CH_3), 1.18 (d,$^{3}J_{H-H}$ = 7.2 Hz, 6H, iPr CH_3); $^{13}C\{^{1}H\}$ NMR (100 MHz, D_2O): δ152.6, 152.3, 141.4, 120.0, 114.9, 104.5, 100.2, 84.2, 83.8, 30.4, 21.1, 17.1.

^{19}F NMR (376.44 MHz, D_2O) δ -72.08 (d, J_{F-P}= 708 Hz)

^{31}P NMR (161.99 MHz, D_2O) δ -145.06 (sept, J_{P-F}= 708 Hz)

HRMS (ESI, H_2O): m/z calculated for $C_{20}H_{23}N_3Ru^{2+}$: 203.5462; m/z measured: 203.5465; $[M+H_2O]^{2+}$: m/z calculated for $C_{20}H_{25}N_3ORu^{2+}$: 212.5515; m/z measured: 212.5515

- Synthesis of [(dpa)Cp*Ir]$(PF_6)_2$ **Ir1'**:

(dpa)Cp*IrO_4S (0.059 g, 0.1 mmol) was weighed into a 20 mL Schlenk tube and dissolved in 2 ml of water. Potassium hexafluorophosphate (0.040 g, 0.22 mmol, 2.2 eq) was added and the

reaction mixture was stirred at room temperature for 30 min. The suspension was filtered by cannula. The resulting solid was washed with cooled water (1 ml) and dried overnight under vacuum to give 0.060 g (yield: 74 %) of the desired product obtained as a yellow solid.

^{1}H NMR (400 Hz, D_2O): δ 8.46-8.45 (m, 2H, CH), 8.04-8.00 (m, 2H, CH), 7.42 (d,$^{3}J_{H-H}$ = 8.4 Hz, 2H, CH), 7.36-7.33 (m, 2H, CH), 1.48 (s, 15H, Cp* CH_3); $^{13}C\{^{1}H\}$ NMR (100 MHz, D_2O): δ 151.0, 150.5, 141.9, 121.5, 115.2, 88.2, 7.7.

^{19}F NMR (376.44 MHz, D_2O) δ -72.09 (d, J_{F-P}= 708 Hz)

^{31}P NMR (161.99 MHz, D_2O) δ -145.05 (sept, J_{P-F}= 708 Hz)

HRMS (ESI, H_2O): m/z Calculated for $C_{20}H_{24}N_3Ir$: 249.5794; m/z measured: 249.5791

- Synthesis of $[(bdpa)Cp^*Ir](PF_6)_2$ **Ir2'**:

With the same procedure as for the synthesis of **Ir1'**, **Ir2'** was obtained as a yellow powder (yield: 82 %). ^{1}H NMR (400 MHz, D_2O) δ 8.61-8.59 (m, 2H, CH), 7.98-7.94 (m, 2H), 7.53-7.37 (m, 9H, CH), 5.54 (s, 2H, CH_2), 1.49 (s, 15H, Cp* CH_3); ^{13}C NMR (100 MHz, D_2O) δ 153.9, 151.0, 142.3, 134.3, 129.0, 128.0, 126.6, 122.5, 116.8, 88.3, 56.3, 7.7.

^{19}F NMR (376.44 MHz, D_2O) δ -72.12 (d, J_{F-P}= 708 Hz)

^{31}P NMR (161.99 MHz, D_2O) δ -145.07 (sept, J_{P-F}= 708 Hz)

HRMS (ESI, H_2O): m/z calculated for $C_{27}H_{30}N_3Ir^{2+}$: 294.6029; m/z measured: 294.6032; $[M+H_2O-H]^{+}$: m/z calculated for $C_{20}H_{25}N_3OIr^{+}$: 606.2091; m/z measured: 606.2082

- Synthesis of $[(dpa)Cp^*IrH](PF_6)$ **Ir5**

A solution of **Ir1** (0.018 g, 0.03 mmol) and HCOONa (0.816 g, 12 mmol) in degassed H_2O (2 ml) was heated at 70 ^{o}C for 30 min. KPF_6 (0.056 g, 0.03 mmol) was then added to the mixture and the reaction was stirred at r.t. for 0.5 h. The solid was filtrated and washed with degassed

water to obtain a light yellow powder after drying under vacuum (0.014g, 75 %). ^{1}H NMR (400 MHz, DMSO) δ 8.52 (s, 1H, NH), 8.31 (d, $^{3}J_{H-H}$ = 5.6 Hz, 2H, CH), 7.83-7.79 (m, 2H, CH), 7.36-7.27 (m, 2H, CH), 6.91-6.86 (m, 2H, CH), 1.55 (s, 15H, Cp* CH_3), -9.44 (s,1H, Ir-H); ^{13}C NMR (100 MHz, DMSO) δ 154.9, 153.2, 139.9, 119.6, 114.5, 87.8, 9.1.

^{19}F NMR (376.44 MHz, DMSO) δ -70.16 (d, J_{F-P} = 711 Hz)

^{31}P NMR (161.99 MHz, DMSO) δ -144.19 (sept, J_{P-F}= 711 Hz)

HRMS (ESI, H_2O): Dicationic compound detected as the major product m/z (z = 2) calculated for $C_{20}H_{24}N_3Ir$: 249.5794; m/z measured: 249.5797

General experimental procedure for transfer hydrogenation of levulinic acid

Safety: As these reactions generate pressures up to 5 bar, they were carried-out in heavy walled (2.7 mm) Schlenk tubes of small size (h = 11 cm, o.d. = 2 cm) equipped with teflon rotaflow manifold. A mobile polycarbonate safety shield was also installed as a protection equipment.

LA (2 mmol), FA (2-4 mmol), catalyst (0.0005-0.1 mol%), with or without water (0-6mL) were added to a 15 mL Schlenk tube with a Teflon screw cap. The mixture of substrates and catalyst was heated to the desired temperature in less than 15 min. After the reaction, the crude mixtures were analyzed by ^{1}H NMR. Volatile compounds were removed under vacuum and the crude product was purified by column chromatography using petroleum ether / ethyl acetate (3/1; v/v) as eluent.

General experimental procedure for hydrogenation of levulinic acid

Catalyst (0.0005-0.1 mol%), levulinic acid (2 mmol) and water (0.5-4 ml) were placed in a 20 ml high pressure Parr reactor. Low catalyst loadings requiring less than 1 mg of catalyst (loading < 0.1 mol%) were realized by dilution of the catalyst in water. The reactor was flushed with H_2 and then pressurized with stirring with the mentioned hydrogen pressure. Once the pressure

reached the reactor was maintained connected for an additional 2 minutes before closing. The mixture was stirred at the appropriate temperature for desired time. After the reaction, the reactor was cooled down in an ice bath and carefully depressurized. The product mixture was analyzed by ^{1}H NMR. The crude product was purified by column chromatography using petroleum ether / ethyl acetate (3/1; v/v) as eluent.

Control experiments where performed by running reactions under the above mentioned conditions without any catalyst.

Dehydration of carbohydrate biomass and subsequent hydrogenation

Glucose or fructose (0.45 g, 2.5 mmol) was loaded into a 20 mL autoclave, and H_2SO_4 (2.5 mL, 0.5 mol/L) was then added. The autoclave was quickly heated to 180 ^{o}C, and vigorously stirred for 2 h. After the reaction, the insoluble solid byproducts were removed by filtration. The hydrolysis filtrate containing LA and FA was transferred to a 20 mL autoclave containing the desired amount of catalyst Ir1 (0.001 mol%). The reaction was then heated at 130 ^{o}C with 5 bar H_2 for 32 h. Finally, the crude product was purified by column chromatography using petroleum ether / ethyl acetate (3/1; v/v) as eluent.

Dehydration of carbohydrate biomass and subsequent transfer hydrogenation

Glucose (0.45 g, 2.5 mmol) was loaded into a 20 mL autoclave, and H_2SO_4 (2.5 mL, 0.5 mol/L) was then added. The autoclave was quickly heated to 180 ^{o}C, and vigorously stirred for 2 h. After the reaction, the insoluble solid byproducts were removed through filtration. The hydrolysis filtrate containing LA and FA was transferred to a 20 mL autoclave containing desired amount of catalyst Ir1 (0.05 mol%), which was then heated to 110 ^{o}C for 24 h. Finally,

the crude product was purified by column chromatography using petroleum ether / ethyl acetate (3/1; v/v) as eluent.

Recycling of Ir1

Ir1 (0.001 mol%), levulinic acid (2 mmol) and water (2 ml) were placed in a 20 ml autoclave. The autoclave was flushed with H_2 and then pressurized to 5 bar. The mixture was stirred at 110 ^{o}C for 32 h. After the reaction, the reactor was cooled down in an ice bath and slowly depressurized. The product mixture was extracted by Et_2O (3x10 ml), the organic phases were collected, concentrated and purified by column chromatography using petroleum ether / ethyl acetate (3/1; v/v) as eluent. The aqueous solution containing **Ir1** was reused in 2 subsequent runs repeating the above mentioned procedure.

AUTHOR INFORMATION

Corresponding Author

* Dr. Cédric Fischmeister

UMR 6226 CNRS. Institut des Sciences Chimiques de Rennes. Université de Rennes 1. Rennes. France

cedric.fischmeister@univ-rennes1.fr

The authors declare no competing financial interests.

Author Contributions

The manuscript was written through contributions of all authors. All authors have given approval to the final version of the manuscript.

ACKNOWLEDGMENT

The authors acknowledge the China Scholarship Council for a grant to SW. The authors would like to acknowledge a reviewer for providing constructive remarks.

ABBREVIATIONS

Dpa, dipyridylamine; LA, levulinic acid; FA, formic acid; GVL, gamma-valerolactone; Cp*, pentamethylcyclopentadienyl;

REFERENCES

[1] (a) van Putten, R.-J.; van der Waal, J. C.; de Jong, E.; Rasrendra, C. B.; Heeres, H. J.; de Vries, J. G. *Chem. Rev*. **2013**, *113*, 1499-1597. (b) Farrán, A.; Cai, C.; Sandoval, M.; Xu, Y.; Liu, J.; Hernáiz, M. J.; Linhardt, R. J. *Chem. Rev*. **2015**, *115*, 6811-6853. (c) Kamm, B. *Angew. Chem., Int. Ed*. **2007**, *46*, 5056-5058. (d) Deuss, P. J.; Barta, K. ; de Vries, J. G. *Catal. Sci. Technol*. **2014**, *4*, 1174-1196. (e) Alonso, D. M.; Wettstein, S. G.; Dumesic, J. A. *Chem. Soc. Rev*. **2012**, *41*, 8075-8098. (f) Li, C.; Zhao, X.; Wang, A.; Huber, G. W.; Zhang, T. *Chem. Rev*. **2015**, *115*, 11559-11624. (g) Climent, M. J.; Corma, A.; Iborra, S. *Green Chem*. **2014**, *16*, 516-547.

[2] (a) Pileidis, F. D.; Titirici, M.-M. *ChemSusChem* **2016**, *9*, 562-582. (b) Werpy, T.; Petersen, G. R.; TopValue Added Chemicals from Biomass. Volume I - Results of Screening for Potential Candidates from Sugars and Synthesis Gas, U. S. D. o. Energy, **2004**. (c) Bozell, J. J.; Petersen, G. R. *Green Chem*. **2010**, *12*, 539-554.

[3] (a) Liguori, F.; Moreno-Marrodan, C.; Barbaro, P. *ACS Catal*. **2015**, *5*, 1882-1894. (b) Fábos, V.; Lui, M. Y.; Mui, Y. F.; Wong, Y. Y.; Mika, L. T.; Qi, L.; Cséfalvay, E.; Kovács, V.; Szűcs, T.; Horváth, I. T. *ACS Sustainable Chem. Eng*. **2015**, *3*, 1899-1904. (c) Caretto, A.; Noè, M.; Selva, M.; Perosa, A. *ACS Sustainable Chem. Eng*. **2014**, *2*, 2131-2141.

[4] (a) Yuan, J.; Li, S.-S.; Yu, L.; Liu, Y.-M.; Cao, Y.; He, H.-Y.; Fan, K.-N.; *Energy. Environ. Sci.* **2013**, *6*, 3308-3313. (b) Cao, W.; Luo, W.; Ge, H.; Su, Y.; Wang, A.; Zhang, T.; *Green Chem.* **2017**, *19*, 2201-2211. (c) Hengst, K.; Ligthart, D. A. J. M.; Doronkin, D. E.; Walter, K. M.; Kleist, W.; Hensen, E. J. M.; Grunwaldt, J.-D. *Ind. Eng. Chem. Res*. **2017**, *56*, 2680−2689 (d) Wright, W. R. H.; Palkovits, R. *ChemSusChem* **2012**, *5*, 1657-1667. (e) Patankar, S. C.; Yadav, G. D. *ACS Sustainable Chem. Eng*. **2015**, *3*, 2619-2630. (f) Ruppert, A. M.; Jędrzejczyk, M,; Sneka-Płatek, O.; Keller, N.; Dumon, A. S.; Michel C.; Sautet, P.; Grams, J. *Green Chem*. **2016**, *18*, 2014-2018. (g) Cui, J.; Tan, J. ; Deng, T.; Cui, X.; Zheng, H.; Zhu, Y.; Li, Y. *Green Chem*. **2015**, *17*, 3084-3089.

[5] Joó, F.; Tóth, Z.; Beck, M. T. *Inorg. Chim. Acta*, **1977**, *25*, L61-L62.

[6] Omoruyi, U.; Page, S.; Hellett, J.; Miller, P. W. *ChemSusChem* **2016**, *9*, 2037-2047.

[7] Tukacs, J. M.; Novák, M. ; Dibó, G.; Mika, L. T. *Catal. Sci. Technol*. **2014**, *4*, 2908-2912.

[8] Li, W.; Xie, J.-H.; Lin, H., Zhou, Q.-L. *Green Chem*. **2012**, *14*, 2388-2390.

[9] Deng, J.; Wang, Y.; Pan, T.; Xu, Q.; Guo, Q.-X., Fu, Y. *ChemSusChem* **2013**, *6*, 1163-1167.

[10] (a) Mehdi, H.; Fábos, V.; Tuba, R.; Bodor, A.; Mika, L. T.; Horváth, I. T. *Top. Catal.* **2008**, *48*, 49-54. (b) Deng, L.; Li, J.; Lai, D.-M.; Fu, Y.; Guo, Q.-X. *Angew. Chem. Int. Ed*.,

2009, *48*, 6529-6532. (c) Heeres, H.; Handana, R.; Chunai, D.; Rasrendra, C. B.; Girisuta, B.; Heeres, H. J. *Green Chem*. **2009**, *11*, 1247-1255. (d) Qi, L.; Horváth, I. T. *ACS Catal*. **2012**, *2,* 2247-2249.

[11] Fábos, V.; Mika, L. T.; Horváth, I. T. *Organometallics*, **2014**, *33*, 181-187.

[12] (a) Romain, C.; Gaillard, S.; Elmkaddem, M. K.; Toupet, L.; Fischmeister, C.; Thomas, C. M.; Renaud, J.- L. *Organometallics*, **2010**, *29*, 1992-1995 (b) Wang, S.; Dorcet, V.; Roisnel, T.; Bruneau,C.; Fischmeister, C. *Organometallics*, **2017**, *36*, 708-713.

[13] (a) Jessop, P. G.; Morris, R. H. *Coord. Chem. Rev*. **1992**, *121*, 155-284. (b) Clapham, S. E.; Hadzovic, A.; Morris, R. H. *Coord. Chem. Rev*. **2004**, *248*, 2201-2237.

[14] (a) Himeda, Y.; Onozawa-Komatsuzaki, N.; Miyazawa, S.; Sugihara, H.; Hirose, T.; Kasuga, K. *Chem. Eur. J.* **2008**, *14*, 11076-11081. (b) Himeda, Y. *Green Chem.*, **2009**, 11, 2018–2022. (c) Wang, W-H.; Hull, J. F.; Muckerman, J. T.; Fujita, E.; Hirose, T.; Himeda, Y. *Chem. Eur. J.* **2012**, *18*, 9397-9404. (d) Wang, W-H.; Muckerman, J. T.; Fujita, E.; Himeda, Y. *ACS Catal*. **2013**, *3*, 856-860.

[15] For examples of dicationic complexes with different counter-anions, see: (a) Ogo, S.; Makihara, N.; Kaneko, Y.; Watanabe, Y. *Organometallics* **2001**, *20*, 4903-4910. (b) Ogo, S.; Kabe, R.; Hayashi, H.; Harada, R.; Fukuzumi, S. *Dalton Trans*. **2006**, *39*, 4657-4663. (c) Kawahara, R.; Fujita, K.-I.; Yamaguchi, R. *Angew. Chem. Int. Ed.* **2012**, *51*, 12790-12794. (d) Brewster, T. P.; Miller, A. J. M.; Heinekey, D. M.; Goldberg, K. I. *J. Am. Chem. Soc*, **2013**, *135*, 16022-16025. (e) Wang, R.; Ma, J.; Li, F. *J. Org. Chem*. **2015**, *80*, 10769−10776; (f) Fujita, K.-I.; Kawahara, R.; Aikawa, T.; Yamaguchi, R. *Angew. Chem. Int. Ed.* **2015**, *54*, 9057–9060.

[16] For a report presenting a zwitterionic structure such as **Ir3**, see: Parent, A. R.; Brewster, T. P.; De Wolf, W.; Crabtree, R. H.; Brudwig, G. W. *Inorg. Chem*. **2012**, *51*, 6147-6152

[17] (a) Hull, J. F.; Himeda, Y.; Wang, W-H.; Hashiguchi, B.; Periana, R.; Szalda, D. J.; Muckerman, J. T.; Fujita, E. *Nature Chem*. **2012**, 4, 383-388. (b) Wang, Z.; Lu, S.-M.; Li, J.; Wang, J.; Li, C. *Chem. Eur. J*. **2015**, *21*, 12592-12595. (c) Barret, S. M.; Slattery, S. A.; Miller, A. J. M. *ACS Catal*. **2015**, *5*, 6320-6327. (d) Mellmann, D.; Sponholz, P.; Junge, H.; Beller, M. *Chem. Soc*. *Rev*. **2016**, *45*, 3954-3988.

[18] (a) Rohmann, K.; Kothe, J.; Haenel, M. W.; Englert, U.; Hölscher, M.; Leitner, W. *Angew. Chem. Int. Ed*. **2016**, *55*, 8966-8969. (b) Wang, W. H.; Himeda, Y.; Muckerman, J. T.; Manbeck, G. F. Fujita, *Chem. Rev.* **2015**, 115, 12936-12973.

[19] For an exemple of hydrogenation in acidic media at 100 bar, see: Moret, S.; Dyson, P. J.; Laurenczy, G. *Nat. Commun*. **2014**, *5*, 4017.

[20] (a) Gladysz J. A. *Chem. Rev*. **2002**, *102*, 3215-3216; (b) Gladysz, J. A. *Pure Appl. Chem*. **2001**, *8*, 1319-1324.

[21] Zhang, Z. *ChemSusChem* **2016**, *9*, 156-171.

[22] Antonetti, C. ; Licursi, D.; Fulignati, S. ; Valentini G. ; Raspolli Galletti, A. M. *Catalysts* **2016**, *6*, 196, doi:10.3390/catal6120196

[23] (a) Kubas, G. J. *Proc. Natl. Acad. Sci. USA*, **2007**, *104*, 6901-6907. (b) Morris, R. H. *Can. J. Chem*. **1996**, *74*, 1907-1915.

[24] Schlaf, M.; Lough, A. J.; Maltby, P. A.; Morris, R. H. *Organometallics*, **1996**, *15*, *2270-2278* and references therein.

[25] Hayashi, H.; Ogo, S.; Fukuzumi, S. *Chem. Commun*. **2004**, 2714-2715.

[26] Tukacs, J. M.; Király, D.; Strádi, A.; Novodarszki, G.; Eke, Z.; Dibó, G.; Kégl, T.; Mika, L. T. *Green Chem.* **2012**, *14*, 2057-2064

[27] Amenuvor, G.; Makhubela, B. C. E.; Darkwa, J. *ACS Sustainable Chem. Eng*. **2016**, *4*, 6010-6018.

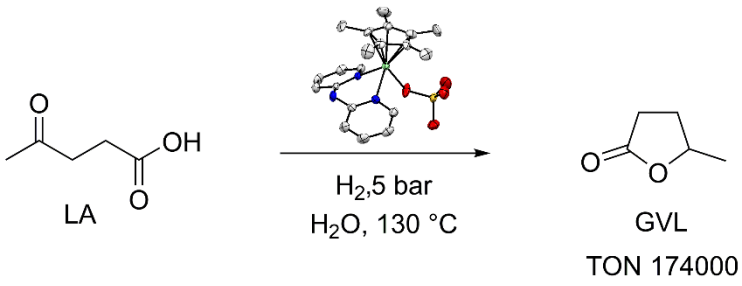

TOC/GA scheme